Paper

Weighted Separation of Surface Reflection of an Object Illuminated By Two Light Sources

（二つの点光源照射による物体表面の反射成分の重み付き分離法）

Xiaohua Zhang (member)†, Kiichi Kobayashi (member)††, Suguru Saito†††, Masayuki Nakajima (member)†††

Abstract Separating the diffuse and specular components from the reflection of a 3D object surface is very important for generating highly realistic synthesized images in computer graphics applications. Most research on this separation has considered only the case in which an object is illuminated by a single point light source. However, when an object is illuminated by one source, it can be difficult or impossible to acquire the real texture information of some visible regions on the object surface because of shading. To overcome this problem, we used two point light sources to illuminate the object to reduce the shaded regions. We used an iterative algorithm to estimate the intensity variation curve parameters and to compute the separation of the two components. To improve the separation quality, we used a weighting function to reduce the effect of noise contained in the highlight regions. Experiments using both synthesized and real data demonstrated that our method is effective and produces clear separation.

Key words: surface reflectance, diffuse reflection, specular reflection, reflection model, weighting function, two light sources

1. Introduction

The separation of the diffuse and specular components from the reflection of an object's surface is very important for generating highly realistic synthesized images in computer graphics applications[1] such as in digital catalogs for on-line sales and digital content for TV program production. For most materials, reflection component separation methods can be categorized into those that work well for objects with a uniform color or multiple colors and those that work well for objects with complicated textures. Research on this separation initially concentrated on the separation of components in the reflection from a uniformly colored object or a multiple-colored object. For uniformly colored objects, separation is done using color space analysis, which partitions a color histogram into clusters to enable computation[2)~4)]. For multiple-colored objects, separation is done using two-dimensional chromaticity space analysis rather than three-dimensional color space analysis[7].

Received July 2, 2003; Revised January 1, 2022; Accepted January 1, 2022

† Hiroshima Institute of Technology
(2-1-1, Miyake, Saeki-ku, Hiroshima, 731-5193, Japan)
†† NHK Engineering Services Inc.
(1-10-11, Kinuta, Setagaya-ku, Tokyo, 157-8510, Japan)
††† Tokyo Institute of Technology
(2-12-1, Ookaya, Meguro-ku, Tokyo, 152-8550, Japan)

However, most objects have complicated textures, and these two methods are not suitable for separating the components in the reflections from objects with complicated textures. Several methods have been proposed for separating the components in the reflections from objects with complicated textures. They can be roughly divided into three categories: polarization based, photometric stereo based, and image sequence based.

Nayar et al. used polarization to separate the reflection components[5]. They assumed that diffuse reflection tends to be unpolarized while specular reflection tends to be partially polarized. In their method, several images are taken of each 3D point on the object while the angle of the polarization filter is rotated. The components are then separated by analyzing the images from the different filter angles.

Woodham et al. used a photometric stereo[9] method in which global and local highlight analysis is used to remove the specular component from the reflection[6)8)]. Other separation methods include using sequential color images to obtain a sequence of sample data for each 3D point on the object surface and using a reflection model to fit the sampled data and compute the reflectance parameter of each point[10)~12)].

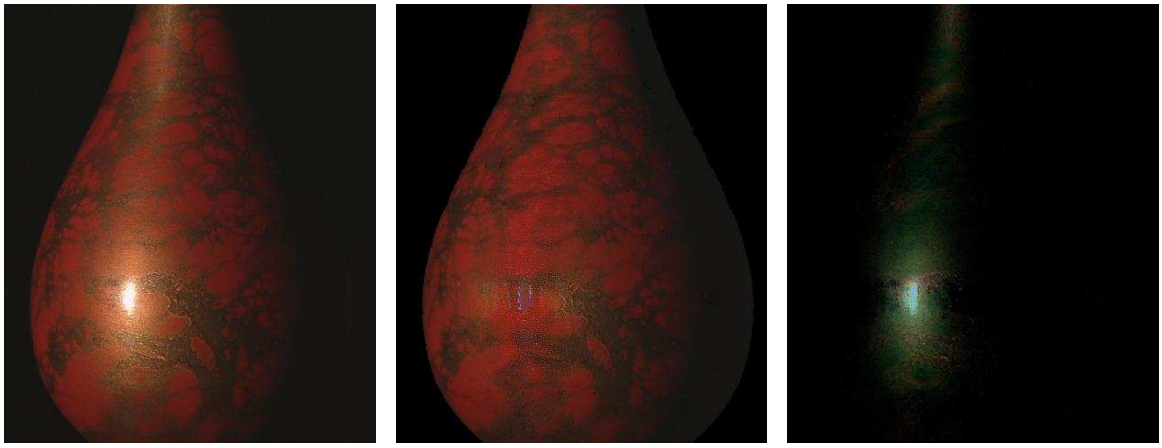

(a) (b) (c)

Fig. 1 Example experimental images of vase surface illuminated by single light source: (a) original image; (b) separated diffuse component; (c) separated specular component. Note that the separation is incomplete, especially around the highlight area and that the texture in the shaded region on the right side was unobtainable.

Our group previously developed a separation method [13] based on a sequence of color images. We estimated the parameters of a reflection model from an intensity image sequence to reduce the errors produced during separation. This enables more effective and stable recovery because the fitting is directly based on the raw RGB data used to compute the model parameters. This method is limited, however, because it does not work for shaded regions in the image due to noisy RGB data. We have now enhaced it so that the object is illuminated by two light sources.

2. Reason for Using Two Light Sources

Why use two light sources to illuminate the object's surface? With only one light source, the real texture information of some regions on the surface is difficult or impossible to acquire because of shading, as shown in Fig. 1(a), which was previously published[13]. Although the right region of the object (a vase) is shaded, it can still be viewed from the camera. Since our image-sequence-based separation method relies on the sampled intensity data for a 3D point on the object's surface, all points should be illuminated when the object is rotated around a axis. However, it is very hard to judge whether a point on an object surface is in an illuminated region or in a shaded region. Using data containing samples in the shaded region may lead to an incomplete separation.

It is almost impossible to obtain substantial information about the texture of a shaded region without resorting to other means. For the object shown in Fig. 1(a), we used an iterative method described elsewhere[13] to separate the diffuse and specular components. As shown in Figs. 1(b) and (c), the separation was incomplete around the highlight area. This is because the reflection model was fitted to intensity variation samples containing data from the shaded region. The texture of the shaded region is thus unobtainable.

While illuminating an object surface with more than one light source enables more information to be obtained for acquiring the texture, too many sources makes separation difficult. The optimal number of light sources depends on the complexity of the object shape.

We have modified the previous method[13] for estimating the surface reflectance and for separating the diffuse and specular components from the reflection of an object to handle illumination by two point light sources. An iterative method is used to fit a simplified Torrance-Sparrow model to the reflection variation data. A weighted method for parameter fitting has been added to reduce the contagion effect of noise during computation of the model parameters.

3. Experimental Setup and Data Sampling

The experimental setup for our image-acquisition system is similar to the previous one[13] except for two point light sources on each side of the camera. They were incandescent lamps with identical characteristics. Assuming that the distances between the light sources and the object are sufficiently greater than the object diameter, the lamps can be regarded as point light sources. We eliminated the ambient light in a room and switched on only the two point light sources. Color HDTV image sequences were obtained by rotating a 3D object around

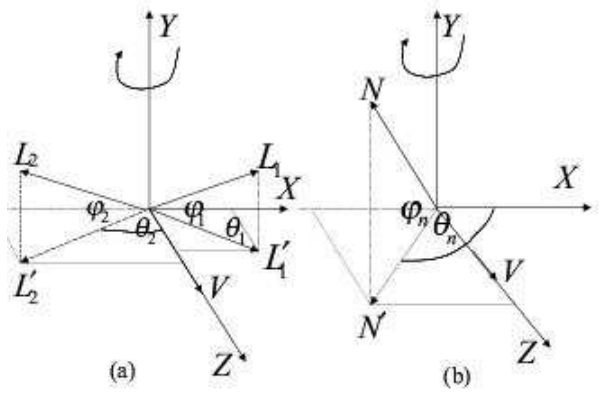

Fig. 2 Geometry of experimental setup: (a) the relationship between light source directions and view direction; (b) the relationship between view direction and normal direction.

its axis of rotation in fixed steps; for example, a step of 2° resulted in a sequence containing 180 images. Prior to image acquisition, the intrinsic and extrinsic parameters of the camera were calibrated for object modeling. The rotation axis of the rotation table was also calibrated to improve the accuracy of the computed model. We used an algorithm similar to Zhang's[14] to calibrate the HDTV camera and a previously developed method to calibrate the rotation axis[15].

Use of the calibrated camera and rotation axis parameters enabled the object model to be computed based on a previously described modeling method[16]. Any pixel on an image can be reprojected onto other images by using the calibrated parameters to obtain the RGB intensity values of the corresponding image pixels. In our experiments, the reprojected pixel was resampled as the average of a small window with a size such as 3×3 pixels to reduce random noise under the assumption that the intensity variation of the image was smooth.

4. Reflectance Properties Estimation

4.1 Reflection Model Using Two Light Sources

Figure. 2 shows the geometry of our experimental setup. To simplify the representation, we drew two diagrams to illustrate the relationships between the light source directions, view direction, and normal direction. Figure 2(a) does not contain the normal vector, while Fig. 2(b) does not contain the light source directions. The vectors shown should be considered to be within the same coordinate system. The optical axis of the camera was collinear with the Z-axis, and the rotation axis of the rotary table was collinear with the Y-axis.

Since object surface reflection can be modeled as a linear combination of the diffuse and specular reflection components for each RGB channel[2)~4)], we use a simplified Torrance-Sparrow model[17] to describe this combination:

$$\begin{aligned}\mathbf{I} &= \mathbf{I}_d + \mathbf{I}_s \\ &= K_d \sum_{i=1}^{2} (\mathbf{L}_i \cdot \mathbf{N}) + K_s \sum_{i=1}^{2} \exp(-\frac{\alpha_i^2}{2\sigma^2}),\end{aligned} \quad (1)$$

where $\mathbf{L} \cdot \mathbf{N}$ is the inner product of two vectors, $\mathbf{L}_i$ are the unit direction vectors of the two light sources, $\mathbf{N}$ is the normal of a 3D point on the object surface, K_d is the diffuse reflection parameter, and K_s is the specular reflection parameter. Parameters α_1 and α_2 are the angles between the surface normal and the bisectors of the light source directions and view direction. The roughness parameter, σ, of a surface is the standard deviation of a facet slope in the Torrance-Sparrow model.

When polar coordinates (φ_1, θ_1) and (φ_2, θ_2) are used to express light directions $\mathbf{L}_1$ and $\mathbf{L}_2$, polar coordinates $(\varphi_n, \theta_n + \theta)$ are used to express the normal vector $\mathbf{N}$ after θ angle rotation. After expansion of Eq. (1), and with some mathematical rearrangement, the diffuse component can be written as a cosine curve equation:

$$\mathbf{I}_d = A \sin\theta + B \cos\theta + C, \quad (2)$$

where θ is the rotation angle of the turntable, and parameters A, B, and C are independent of the rotation angle.

The specular component of intensity variation is often modeled approximately as a Gaussian[10], so we express the specular component of the variation curve as

$$\mathbf{I}_s = D_1 \exp\left(-\left(\frac{E_1-\theta}{F}\right)^2\right) + D_2 \exp\left(-\left(\frac{E_2-\theta}{F}\right)^2\right), \quad (3)$$

where θ is the rotation angle of the turntable, and $F = \sqrt{2}\sigma$. Parameters E_1 and E_2 correspond to the highlight peak positions in the variation curve. Parameters D_1 and D_2 correspond to the specular reflectance, K_s.

4.2 Minimization Problem

The intensity variation curve described in continuous form in Eqs. (2) and (3) can be easily expressed in a discrete form by replacing θ with θ_k, which represents the rotation angle at the time instant (indexed by k) at which intensity $\mathbf{I}_k$ is sampled. The curve parameters in Eqs. (2) and (3) are estimated before separating the reflection components and computing the reflectance parameters.

Using these equations, we can model total reflection as a nonlinear function. We use the Levenberg-Marquardt iterative method[18] to estimate the curve parameters that minimize nonlinear fitting error

$$E = \sum_k \left(\mathbf{I}(\theta_k; A, B, C, D_1, E_1, D_2, E_2, F) - \mathbf{I}_k \right)^2. \quad (4)$$

However, for the reflection from a 3D point on the surface, the specular reflection is more difficult to model than the diffuse reflection. Moreover, because of the camera's limited dynamic range, the highlight region may contain more noise than the diffuse region. Therefore, we use a weighting function to place more weight on the diffuse than the specular reflection components. To this end, we construct a weighting function to be the inverse of the specular reflection:

$$W_{\theta_k} = \left[a + \exp\left(-\left(\frac{E_1 - \theta_k}{F} \right)^2 \right) + \exp\left(-\left(\frac{E_2 - \theta_k}{F} \right)^2 \right) \right]^{-\frac{m}{n}} \quad (5)$$

where constant a is empirically set between 10^{-9} and 10^{-3}; this is only to prevent the weighting function becoming infinite so that it remains numerically meaningful. The integer parameters $m \geqq 0$ and $n > 0$ are used to control the shape of the weighting function. As m becomes larger or n becomes smaller, the dependence of the weighting function on the diffuse component becomes greater. If m/n is very small and approximately zero, the weighting function is approximately 1. In this case, all sample data have almost the same weight.

With a weight on each sample datum, the fitting error (Eq. (4)) can be rewritten as

$$E = \sum_k W_{\theta_k} \left(\mathbf{I}(\theta_k; A, B, C, D_1, E_1, D_2, E_2, F) - \mathbf{I}_k \right)^2. \quad (6)$$

The definition of the above weighting function shows that it depends on the coefficients of the intensity variation curve as well on as the rotation angle. Since we use the Levenberg-Marquardt iterative method to solve Eq. (6), the weights should be adapted for each loop until iteration ends. The initial values of all parameters were set using a method described elsewhere[13].

4.3 Separation of Reflection Components

When the intensity variation curve parameter in Eqs. (2) and (3) have been estimated, the separation of diffuse and specular components becomes simple. One way to solve the separation problem is to use the previously described method[13]. However, if the surface reflection contains very strong specular reflection that overflows the camera's limited dynamic range [0-255], the peak in the intensity variation curve will be flattened in the rotation range and will not be a sharp Gaussian-like peak. Gaussian fitting to the specular components will result in large errors, preventing this method from completely separating the two components. We mentioned that modeling of the diffuse component is more accurate than that of the specular component. Our experiments confirmed that the curve parameters of the diffuse component are more reliable than those of the specular component. Therefore, in our implementation, we simply computed the diffuse component, I_d, using the diffuse reflection model and subtracted it from the sampled data. We used the result as the specular component.

Because of the noise and sampling errors, for a very small number of intensity variation curves, the computed diffuse components were negative. For the corresponding 3D points, the diffuse and specular components were computed using bilinear interpolation. The separation was carried out independently for each RGB channel.

4.4 Computing the Reflectance Parameters

Computing the reflectance parameters requires knowledge of the light directions measured in advance. After estimating the curve parameters, we can calculate the surface normal by combining the parameters with the known light directions.

Using computed normal vector N and measured light source directions L_1 and L_2, we compute the diffuse reflectance parameter:

$$K_d = \frac{I_d}{\max\{L_1 \cdot N, 0\} + \max\{L_2 \cdot N, 0\}}. \quad (7)$$

The computation of the specular reflectance parameter is more difficult than that of the diffuse reflectance parameter. If there is no specular reflection component in the intensity variation curve, one cannot compute the specular reflectance parameter. The following computation is only for 3D points whose intensity variation curves contain specular components. We used only the largest peak to compute the reflectance parameter.

Without loss of generality, suppose $D_1 \geqq D_2$. This means that when the object is rotated E_1 degrees, the specular component reaches its maximum. We denote the bisector between light source direction L_1 and view direction V as L_{b1}. When the specular component reaches its maximum, and if the angle between bisector L_{b1} and the normal vector is β, the specular reflectance can be approximately computed using

$$K_s = D_1 \exp\left(-(\beta / F)^2 \right). \quad (8)$$

We calculated K_s for each RGB channel, while the

(a) (b) (c) (d)

Fig. 3 Example experimental results with synthesized images: (a) image used; (b) separated diffuse component; (c) separated specular component and (d) image representation of diffuse parameter K_d.

normal vector takes the averaged value from three channels.

From the definition of curve parameter F in Eq. (3), roughness parameter σ is approximately given as $\sigma = \sqrt{2}F/2$.

5. Experimental Results

We performed experiments using synthesized and real data obtained from an image sequence to verify the effectiveness of the weighted separation for computing the two components.

Synthesized images: We first synthesized an image sequence of a cylindrical object using a mechanism similar to the real experimental setup through a virtual camera. A texture was mapped onto the surface. Diffuse and specular reflection components were added to images with 640×480 resolution. We took the object shape as unknown and reconstructed it using the modeling method mentioned above[16]. Each 3D point on the surface was reprojected onto images using camera parameters while the object was rotating about its axis. From this, we obtained the intensity variation curve for each 3D point. The sampled data were then fed into our iterative algorithm to compute curve parameters and then the two reflection components were separated and the reflectance parameters were computed.

Figure 3 shows example experimental results for a synthesized image. Note that the value of diffuse parameter K_d is independent of the light source direction.

Real images: The real images were acquired using the same method described as before[13], except for the two light sources on both sides of the HDTV camera.

Figure 4 shows example experimental results for an real image. Using the method described in section 4.4, we computed the diffuse reflectance parameters, which are represented as an image in Fig. 4(f). This image is independent of the light source direction. Comparison of the images in Figs. 4(d and e) with those in Figs. 1(b and c) shows that the diffuse component of the reflection from an object illuminated by two light sources provides more visual information about the real texture than that of an object illuminated by one light source.

Due to resolution and printing problems, it is difficult to see the difference between the results with weighting (Figs. 4(d) and (e)) and without weighting (Figs. 4(b) and (c)). To demonstrate that weighting improves the results of separation, we show close-ups of the same areas in Figs. 4(g)-(j). Figure (g) is from separated diffuse component (b) without weighting, while (h) is from separated diffuse component (d) with weighting. Careful visual inspection shows that the portions on the left and right of the highlight in (g) appear dirty yellowish while those in (h) are cleaner and coincide with the surface texture of the actual object. The improvement can also be confirmed by visually comparing Fig. 4(i), which is the close-up specular component (c) separated without weighting, with Fig. 4(j), which is the close-up specular component (e) separated with weighting. The component has abrupt variations on the two sides of each highlight area in Fig. 4(i), while the variations in Fig. 4(j) are smoother and coincide with the shape of the actual object.

6. Conclusion

We have developed a method for separating the diffuse and specular components in the reflection from an object illuminated by two light sources. Using two light sources reduces the size of shaded region, enabling sufficient visual information to be obtained for acquiring the texture of the object. A weighting function was used to minimize the incomplete separation due to noise, the camera's limited dynamic range, etc. Our experimental

results show that the proposed method is effective and produces clear separation. We plan to use it in experiments using objects with different shapes and with area light sources.

Acknowledgements

This work was part of a project supported by TAO.

〔References〕

1) F. Bernardi, I. M. Martin, and H. Rushmeier, "High-quality texture reconstruction from multiple scans", IEEE Transactions on Visualization and Computer Graphics, 7, 4, pp. 318-332, (2001)
2) G. J. Klinker, S. A. Shafer, and T. Kanade, "Using a color reflection model to separate highlights from object color", International Conference on Computer Vision, pp. 145-150, (1987)
3) G. J. Klinker, S. A. Shafer, and T. Kanade, "The measurement of highlight in color images", International Journal of Computer Vision (IJCV), 2, 1, pp. 7-32, (1988)
4) G. J. Klinker, S. A. Shafer, and T. Kanade, "A physical approach to color image understanding", International Journal of Computer Vision (IJCV), 4, 1, pp. 7-38, (1990)
5) S. K. Nayar, X. S. Fang, and T. Boult, "Separation of reflection components using color and polarization", International Journal of Computer Vision (IJCV), 21, 3, pp. 163-186, (1997)
6) K. Schluns and O. Wittig, "Photometric stereo for non-Lambertian surfaces using color information", Proceedings of 7th International Conference on Image Analysis and Processing, pp. 505-512, (1993)
7) K. Schluns and M. Teschner, "Fast separation of reflection components and its application in 3D shape recovery", Proceedings of 3rd Color Imaging Conference, pp. 48-51, (1995)
8) Karsten Schluns and Andreas Koschan, "Global and Local Highlight Analysis in Color Images", Proc. 1st Int. Conf. on Color in Graphics and Image Processing (CGIP), pp. 300-304, (2000)
9) R. J. Woodham, Y. Iwahori, and R. A. Barman, "Photometric stereo: Lambertian reflectance and light sources with unknown direction and strength", Technical Report 91-18, (August 1991)
10) Y. Sato and K. Ikeuchi, "Temporal-color space analysis of reflection", Journal of Optical Society of America A, 11, 11, pp. 2990-3002, (November 1994)
11) Y. Sato, M. D. Wheeler, and K. Ikeuchi, "Object shape and reflectance modeling from observation", SIGGRAPH'97, pp. 379-387, (1997)
12) H. Saito, K. Omata, and S. Ozawa, "Recovery of Shape and Surface Reflectance of Specular Object from Rotation of Light Source", 2nd Int'l Conf. on 3D Digital Imaging and Modeling (3DIM99), pp. 526-535, (1999)
13) X. Zhang, Y. Nakanishi, K. Kobayashi, H. Mitsumine, and S. Saito, "Estimation of surface reflectance parameters from image sequences", The Journal of The Society for Art and Science, 1, 1, pp. 8-14, (2002)
14) Z. Zhang, "A flexible new technique for camera calibration", IEEE Trans. on Pattern Analysis and Machine Intelligence, 22, 11, pp. 1330-1334, (Nov. 2000) Also http://research.microsoft.com/users/zhang/
15) X. Zhang, Y. Nakanishi, K. Kobayashi, and H. Mitsumine: "Camera calibration and rotary table calibration using image sequence", Proceedings of the 2001 IEICE Society Conference, p. 223, (2001)
16) K. Kobayashi, Y. Nakanishi, X. Zhang, M. Tadenuma, H. Mitsumine, and S. Saito: "High resolution 3D surface measurement from multiple viewpoint images", NICOGRAPH 2000, pp. 143-150, (2000)
17) K. E. Torrance and E. M. Sparrow, "Theory for Off-specular Reflection from Roughened Surfaces", Journal of the Optical Society of America, (JOSA), 57, pp. 1105-1114, (1967)
18) W. H. Press et al., "Numerical recipes in C: the art of scientific computing", 2nd edition, Cambridge University Press, p. 683, (1992)

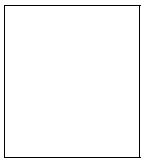

Xiaohua Zhang received a B.S. degree in computing mathematics from JiangXi University, P. R. China, in 1984, an M.S. degree in computer science and engineering from Jinlin University of Technology, P. R. China, in 1990, and a Dr. Eng. degree in information science and engineering from the Tokyo Institute of Technology, Japan, in 2000. After working at NHK Engineering Services Inc. from 2000 to 2003, he joined the faculty of the Hiroshima Institute of Technology. His research interests include computer graphics, image processing, computer vision, and virtual reality.

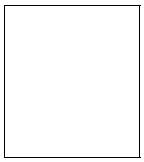

Kiichi KOBAYASHI received B.E. and M.E. degrees in electrical engineering from Keio University, in 1965 and 1967, respectively. He joined NHK (Japan Broadcasting Corp.) in 1967. From 1970 to 1998, he researched MOS devices and designed and developed MOS VLSI technologies for TV signal processing at NHK Technical Research Laboratories. Since 1998, he has researched advanced technologies for TV program production at NHK Engineering Services Inc.

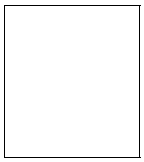

Suguru SAITO received B.S., M.S. and Dr. Eng. degrees in computer science and engineering from the Tokyo Institute of Technology in 1994, 1996, and 1999, respectively. He is now researching computer graphics, image processing, and virtual reality at the Tokyo Institute of Technology.

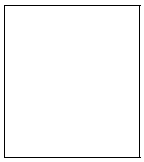

Masayuki NAKAJIMA received B.E.E. and Dr. Eng. degrees from the Tokyo Institute of Technology, Tokyo, Japan, in 1969 and 1975, respectively. Since 1975, he has been with the Department of Imaging Science and Engineering, Tokyo Institute of Technology, Yokohama, Japan. He is now a professor in the Department of Computer Science, the Faculty of the Graduate School of Information Science and Engineering, Tokyo Institute of Technology, Tokyo, Japan. His fields of interest are computer graphics, pattern recognition, image processing, and virtual reality.

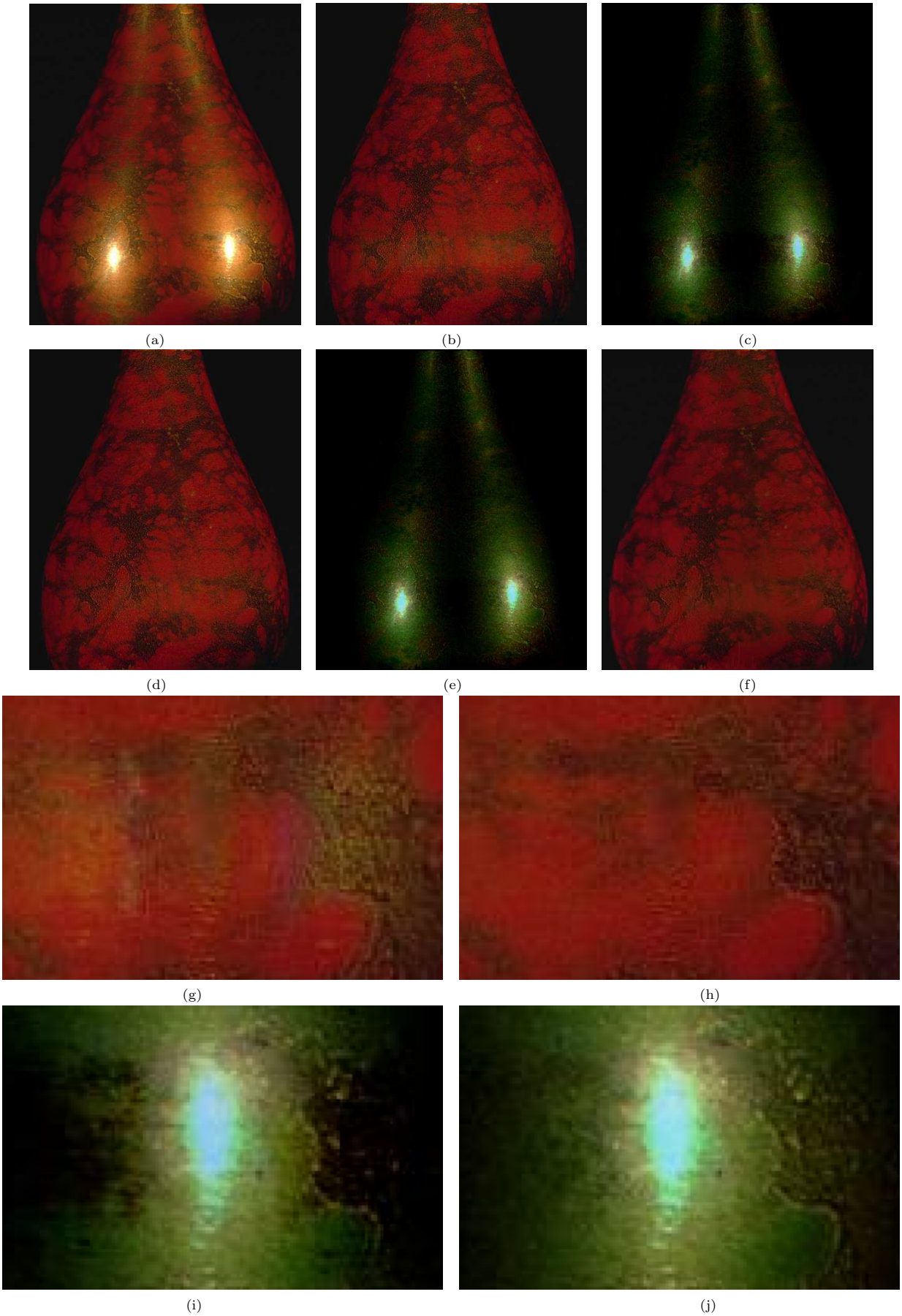

Fig. 4 Example experimental results with real images: (a) image used; (b) and (c) separated diffuse and specular components without weighting; (d) and (e) separated diffuse and specular components with weighting; (f) image representation of diffuse reflectance parameters; and (g), (h), (i), and (j) close-ups of regions containing the right highlight of Figs. (b), (d), (c), and (e).